Automatic Image Colorization using Generative Adversarial Networks

Project Paper of team: Yet Another Layer [YAL]
CSci 5561 - Computer Vision

Cameron Fabbri, Md Jahidul Islam

Abstract

Abstract need to be added Abstract need to be added

1 Introduction

Image colorization [1, 2, 3] refers to colorizing a given gray-scale image so that it appears real. A large amount of photographs, videos and movies, mainly antique, lack color; image colorization can provide a modern and vivid view to these images. In addition, surveillance cameras often capture (or store) gray-scale images for convenience. Several underwater inspection and surveillance applications [4, 5] often have to deal with color-less images due to lack of visible light in deep-water. Robust and efficient image colorization techniques can be used in these applications with substantial benefits.

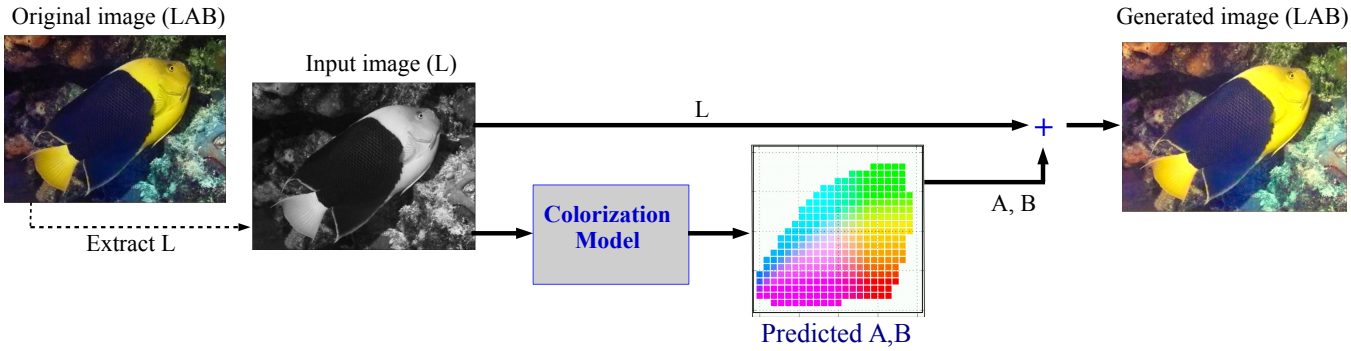

Figure 1: Basic image colorization procedure is shown. LAB color-space is generally used for convenience (*i.e.*, one less unknown dimension); given the lightness channel L, task for the colorization model is to predict A and B channels so that the colorized image appears natural.

Colorizing a gray-scale image (*i.e.*, only intensity values are known) is a difficult and ill-posed problem. Computer vision community have approached this problem in different ways over the last few decades [1, 2, 3, 6, 7, 8]. Before the advent of deep-learning [9], researchers have tried many classical techniques [6, 7, 8, 10, 11] to capture relationships between color components (RGB or LAB) and image level features. Due to multi-modality and ill-posed nature of the problem, optimization based techniques [10, 6] and probabilistic models [11] were the only ones that achieved decent colorization performance in few specific applications. However, overall performance of these techniques, in general, were still poor due to the high non-linearity and abstract nature of color-feature relationship.

Recently, deep-learning based image colorization techniques [1, 2, 12, 13], trained over millions of images, have shown significantly better performance over the earlier classical methods. For instance, the current state-of-the-art, 'colorful colorization' [1], can fool a human observer 32% of the time in a *colorization Turing-test* scenario. **Additionally, how use of GANs are likely to improve the performance which why we are going to try?**

In this project, we *// need to be added. need to be added. need to be added. need to be added. need to be added. need to be added. need to be added. need to be added. need to be added. need to be added. need to be added. need to be added. need to be added. need to be added. need to be added. need to be added. need to be added. need to be added. need to be added.*

2 Background and Related Work

As mentioned in the previous Section, image colorization is an ill-posed problem due to multi-modality and ambiguity. While some natural objects commonly hold the same color (e.g grass is *usually* green), many are left up for interpretation. For example, given a gray-scale image of someone wearing a dark colored shirt, there is no way of figuring out the true color. Instead, the objective is to come up with a colorization that appears real, *i.e.*, natural.

User-based approaches [10, 8, 14, 15] were popular for being fast and relatively accurate as user can provide a good prior for the inherent color distribution. However, these methods are not applicable for large scale automatic colorization, which led researchers to adopt optimization and probabilistic approaches [6, 3, 11]. These approaches model a likelihood based color approximation for each pixel given the neighborhood information. Few methods introduce additional step for spatial coherency through image based segmentation as well. However, overall colorization performance of these approaches are not very appealing [16] for general usage in a large scale. This is because the prior distribution of color-space is domain-dependant; for instance, face images, underwater images, outdoor and satellite images, all have different color distributions. Besides, it is difficult to capture the highly non-linear and abstract color-feature relationships without large-scale training.

In recent times, deep-learning based approaches [1, 2, 12, 13] have produced significantly better colorization performance as they can extract highly non-linear spatial relationships if trained over large datasets. The convolutional layers learn appropriate filters to produce good feature-space representations from raw images. These feature extraction and filtering is performed over multiple layers to capture complex spatial relationships within the image-space, which is useful for image-to-image translation tasks. **Additionally, Prospects of GANs GANs .....**

In this project, we *// need to be added. need to be added. need to be added. need to be added. need to be added. need to be added. need to be added. need to be added. need to be added. need to be added. need to be added. need to be added. need to be added. need to be added. need to be added. need to be added. need to be added. need to be added. need to be added.*

3 Generative Approaches

In our project, we tried two classical methods: *colorization using optimization* [10], *colorization via multimodal predictions* [6]. The former is not an automatic approach (user provides color distribution prior), whereas, the later uses a set of reference images to formulate color distribution. Their operations are discussed in our term report; this paper focuses on the third generative approach, *colorful image colorization* [1], which is adopted in our project.

3.1 Adopted Model: Colorful Image Colorization

Colorful image colorization [1] is considered as a major breakthrough on this problem. Published on 2016, it has managed to set a new benchmark for performance. It is an automatic approach that produces realistic colorizations based on a CNN-based model. It poses the problem as a multi-modal classification problem. The objective function is carefully designed to map the image-to-image translation problem to a classification problem. First, it takes advantage of the fact that A, B color components of LAB colorspace for natural images are concentrated in a small region, which are discretized into finite number of bins (Q). Given the lightness channel (L_p) of a pixel p, its A, B pair corresponds to a particular bin (out of 313 bins in total), which is mapped to a 1-hot vector (Z_p). Consequently, task of the classification model, is to predict which bin each pixel corresponds to. That is, the output is a 313-mode probability distribution ($\hat{Z}_p$) for each pixel p. The objective function is modelled as a cross entropy loss between Z and $\hat{Z}$, expressed as follows:

$$L_{col}(Z, \hat{Z}) = -\sum_{p} Z_p \sum_{q \in Q} Z_p[q] log(\hat{Z}_p[q])$$

This cross-entropy loss is further augmented with class rebalancing, to encourage rare colors. The detailed model specification, as shown in Fig. 2, is an 8-layer CNN architecture where each conv layer refers to a block of 2 or 3 repeated conv and ReLU layers [17], followed by a BatchNorm layer [18]. The network has no pool layers; all changes in resolution are achieved through spatial down-sampling or up-sampling between conv blocks.

3.2 Implementation Details and Model Changes

While working on designing a generator for our GAN-based model, we investigated this model with different objective functions (L_1 loss, L_2 loss, least-squared loss, etc.) instead of their cross-entropy based loss function. This is due to the fact that in a GAN-based model, *discriminator* expects an image from the *generator*, and tries to discriminate it as real or fake in order to force the generator to get better. Therefore, rather than adopting their classification model directly, we implemented their architecture using objective functions based on L_1, L_2, least-squared loss (so that it outputs an image, not classification probabilities). Additionally, it made our model end-to-end trainable, which can be easily incorporated in a GAN-based architecture.

Given an input image I, the network is fed with its L channel (I_L); the output layer of the network is adjusted to predict $\hat{I}_{AB}$. We have found L_1 and L_2 loss functions perform quite well with this model. These loss functions between true I_{AB} and $\hat{I}_{AB}$ can be expressed as follows:

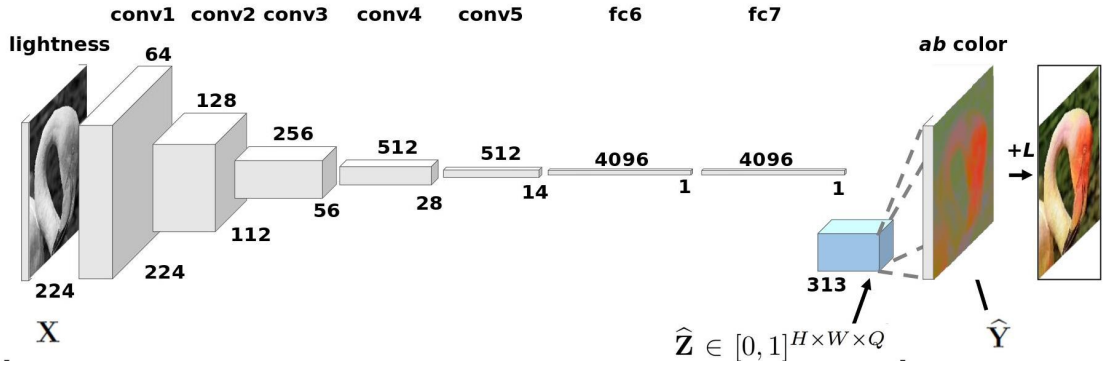

Figure 2: Architecture of colorful image colorization model [1] that is adopted in our evaluation

$$L_1(I_{AB}, \hat{I}_{AB}) = \lambda \sum_p |I_{AB}[p] - \hat{I}_{AB}[p]|$$

$$L_2(I_{AB}, \hat{I}_{AB}) = \lambda \sum_p (I_{AB}[p] - \hat{I}_{AB}[p])^2$$

Here, λ is a normalization constant. CelebA datasets [19] is used for training primarily, that has $195K$ training examples (a total of $202K$ images); In a separate training, a set of $200K$ images from Places2 dataset [20] were also used for training[1]. Training was performed using two 1080 gpus (in a core-i7 machine having 64GB RAM); training time for $100K$ iterations with a batch size 32 was about 2-3 days for each trial. The implementation is done using TensoFlow [22] in python.

3.3 Results

We found that this model performs better with L_1 loss function compared to L_2 loss. This might be because of the averaging effect of 2-norm which causes a blurry colorization (similar phenomena is discussed in [1]). The results on few test cases are shown in Fig. 3.

In the results state above, colorful colorization model is used as a generator only (**Col. Col. (G)**); we also used this model as a generator in a GAN (**Col. Col. (GAN)**) to investigate its performance. As illustrated in Fig. 3(c), images colorized by Col. Col. (GAN) are more realistic and consistent than Col. Col. (G). In addition, we provided results obtained by colorization via multi-modal prediction [6] to demonstrate the degree of improvements using colorful colorization model.

The colorful colorization model, as a generator alone, and as a generator in a GAN, achieve decent colorization performance. Next, we discuss other GAN based models for image colorization, which we investigated in our project.

4 Adversarial Approaches

Generative Adversarial Networks (GANs) [REF] are a recent class of generative models based on game theory in which a generator network is pitted against an adversary. The adversary or discriminator, D, is a neural network trained to discriminate between real samples and samples generated by the generator. The generator, G, is trained to fool the adversary. They have shown very impressive results towards various tasks including inpainting, domain adaptation, and image colorization. Due to the difficulty in training them in practice, there have been several theoretical approaches towards stabalizing their training by providing better gradients for the generator in terms of changing the loss function for the discriminator. Regular GANs modeled the discriminator as a classifier with the sigmoid cross entropy loss function, which has been shown to suffer from the vanishing gradient problem [REF]. We experimented with four different variations of GANs: Regular GANs, Least Squares GANs (LSGAN), Energy-Based GANs (EBGAN), and Wasserstein GAN (WGAN). There has been little work in using GANs for the task of image colorization. Most notable is the Pix2Pix model which uses the normal GANs loss, but also show that often their generator fails to generate any color at all. We hypothesize that in comparison to the common task in which GANs are trained to generate an image from a noise prior, the discriminator for the task of colorization has a much more difficult job due to the visual similarity between images. For this reason, a much stronger discriminator is needed, but as shown in [REF], with the normal GANs loss, as the discriminator gets better, the gradients passed to the generator, and therefore the generator itself, become worse. For this reason we chose to explore other options for the discriminator loss. Our model is set up as a *conditional* GAN (cGAN), in which the generator is conditioned on the grayscale image. The rest of this section compares the different GAN formulations, and ends with our architecture designs. We combine the GAN objective with L_1 and L_2 in order to provide some sense of ground truth. These can be expressed as:

[1]Larger datasets like ImageNet [21] and full Places2 challenge dataset were not used for the project due to time constraint; however, we are planning to train our final GAN-based model over these datasets during the summer.

(a) Colorful Colorization [1] model with L1 loss

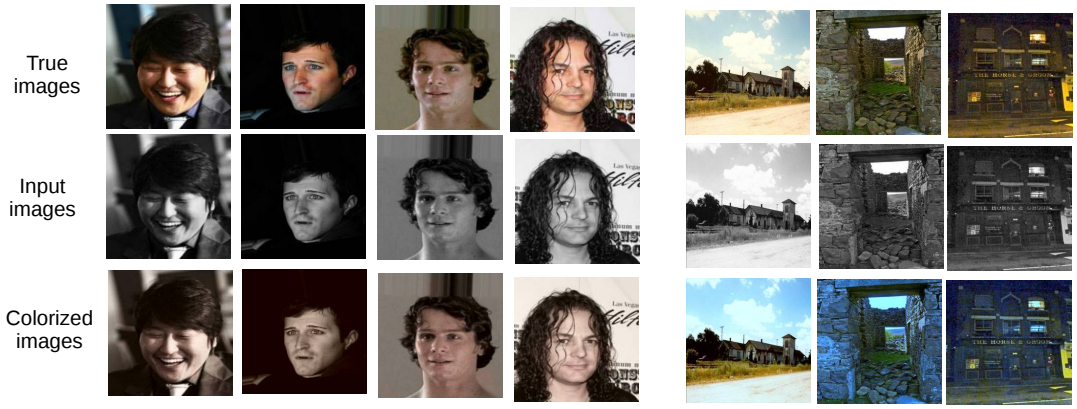

(b) Colorful Colorization [1] model with L2 loss

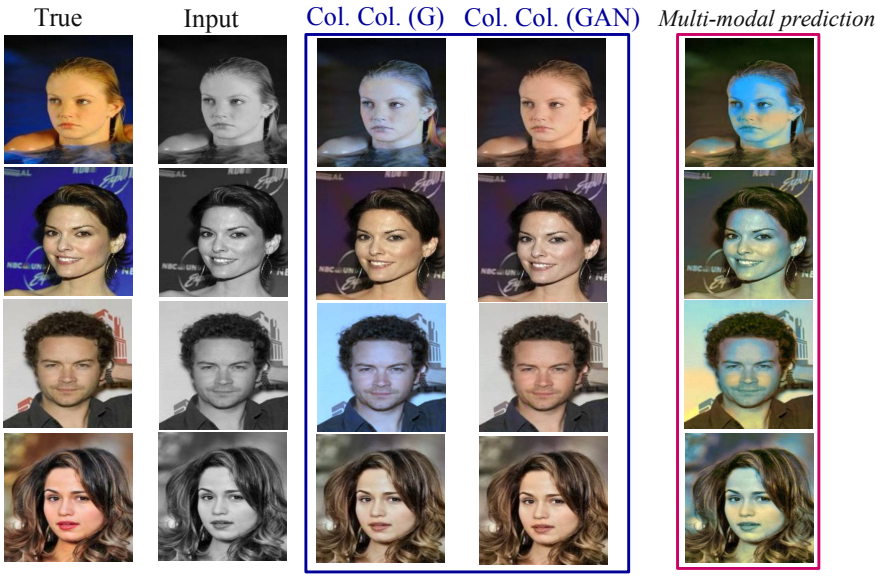

(c) Results in comparison with different models

Figure 3: Results for the colorful colorization model [1] with (a) L1 and (b) L2 loss is shown; First 4 columns show few examples from the test set of CelebA [19] dataset, while the rest (3) columns correspond to Places2 [20] dataset. Comparison for colorful colorization model used as a generator only (Col. Col. (G)), and as a generator in a GAN (Col. Col. (GAN)), is shown in (c); also, results obtained by colorization via multi-modal prediction [6] is provided in the last column to demonstrate the degree of improvements using colorful colorization model.

$$\mathcal{L}_{L_1}(G) = \mathbb{E}_{x,y\sim p_{data}(x,y)}[||y - G(x)||_1]$$
$$\mathcal{L}_{L_2}(G) = \mathbb{E}_{x,y\sim p_{data}(x,y)}[(y - G(x))^2]$$

These are able to capture low frequencies, but have been shown to lack in capturing high frequencies, resulting in blurry images in the case of autoencoders, or saturated colors in the case of colorization. These imperfections should in theory be rejected by the discriminator, which results in successfully capturing high frequencies in images such as sharp edges

and bright colors. Note that using these losses along with the GAN loss does not change the discriminator's objective, it is the generator that is required to fool the discriminator as well as be near the ground truth.

4.1 DCGANs

Because of the high dimensionality and spacial structure of images, we chose to use Deep Convolutional GANs (DCGANs), which take advantage of the recent successes of Convolutional Neural Networks (CNN) as part of their architecture, as opposed to the simple neural networks used in [GAN PAPER]. The objective function is given as:

$$\min_G \max_D \mathbb{E}_{x \sim p_{data(x)}}[logD(\boldsymbol{x})] + \mathbb{E}_{z \sim p_z(z)}[log(1 - D(G(z)))]$$

where p_{data} represents the true data, and p_z represents some noise prior, e.g. $z \sim \mathcal{N}$. for our conditional DCGAN can be expressed as:

$$\mathcal{L}_{DCGAN}(G, D) = \mathbb{E}_{x,y \sim p_{data}} logD(x, y) + \mathbb{E}_{x \sim p_{data}} log(1 - D(x, G(x)))$$

where x represents the grayscale image, and y represents the ab color values associated with x. Combining this with our L_1 and L_2 loss functions gives us our final objective:

$$G^* = \lambda_1 \mathcal{L}_{DCGAN} + \lambda_2 \mathcal{L}_{L_1} + \lambda_3 \mathcal{L}_{L_2}$$

where λ_1, λ_2, and λ_3 are hyperparameters. One should note that z is discarded in this formulation, resulting in a deterministic model. Because of the high volume of information given in the grayscale image in comparison to something like conditioning on a class label, we believe the model would simply learn to discard z as noise (because that's quite literally what it is). Instead, we provide noise in the form of droupout in the generator, but have not seen much difference in the output. We evaluated our method on the CelebA dataset. Some results can be seen in Figure X.

4.2 LSGANs

Least Squares GANs (LSGANs) provide a least squares loss for the discriminator in order to penalize samples that may have fooled the discriminator but do not lie close to the true data distribution. The objectives for conditional LSGANs are defined as:

$$\min_D V_{cLSGAN}(D) = \frac{1}{2}\mathbb{E}_{x,y \sim p_{data(x,y)}}[(D(x, y) - b)^2] + \frac{1}{2}\mathbb{E}_{x \sim p_{data}}[(D(G(x)) - a)^2]$$

$$\min_G V_{cLSGAN}(G) = \frac{1}{2}\mathbb{E}_{x \sim p_{data(x)}}[(D(G(x)) - c)^2]$$

where $a = 0$ to denote the fake data, $b = 1$ to denote the true data, and $c = 1$ in order to try and fool D.
where p_{data} represents the true data, x represents the grayscale image, y represents the corresponding ab color channels for x. We combine the LSGAN objective with L_1 and L_2 to give our final objective:

$$G^* = \lambda_1 V_{cLSGAN} + \lambda_2 \mathcal{L}_{L_1} + \lambda_3 \mathcal{L}_{L_2}$$

where λ_1, λ_2, and λ_3 are hyperparameters. We evaluated LSGANs on the CelebA dataset. Some results can be seen in Figure X.

4.3 EBGANs

Energy-Based GANs (EBGANs) model the discriminator as an energy function that attributes low energies to the regions near the data manifold and higher energies to other regions. Unlike the other GAN variations mentioned, the EBGANs discriminator is modeled as an autoencoder, which aims to provide a more diverse set of outputs as opposed to the binary logistic loss. The objectives for conditional EBGANs are defined as:

$$\mathcal{L}_{cEBGAN} D(x, y) = D(x, y) + max(0, (m - D(G(z))))$$

$$\mathcal{L}_{cEBGAN} G(x) = D(G(x))$$

where m is some margin, x represents the grayscale image, y represents the corresponding ab color channels for x. We combine the EBGAN objective with L_1 and L_2 to give our final objective:

$$G^* = \lambda_1 \mathcal{L}_{cEBGAN} + \lambda_2 \mathcal{L}_{L_1} + \lambda_3 \mathcal{L}_{L_2}$$

where λ_1, λ_2, and λ_3 are hyperparameters. We evaluated EBGANs on the CelebA dataset. Some results can be seen in Figure X.

4.4 WGAN

The Wasserstein GAN (WGAN) approximates the Earth Mover (EM) distance given a set of K-Lipschitz functions f. In order to have the parameters w lie in a compact space and ensure f is K-Lipschitz, the weights of the network are clamped to some range. Because the EM distance is continuous and differentiable, the discriminator (critic) should be trained to optimality, which offers better gradients to the generator. This offers stable training at the expense of slow training, because the critic must be updated multiple times for one update of the generator. Our conditional WGAN objective function is:

$$\mathcal{L}_{cWGAN} = \max_{w \in W} \mathbb{E}_{x,y \sim \mathbb{P}_{data}}[f_w(x, y)] - \mathbb{E}_{x \sim p_{data}}[f_w(G(x))]$$

where x represents the grayscale image and y represents the corresponding ab color channels for x. We combine the WGAN objective with L_1 and L_2 to give our final objective:

$$G^* = \lambda_1 \mathcal{L}_{cWGAN} + \lambda_2 \mathcal{L}_{L_1} + \lambda_3 \mathcal{L}_{L_2}$$

where λ_1, λ_2, and λ_3 are hyperparameters. We evaluated WGAN on the CelebA dataset. Some results can be seen in Figure X.

5 Conclusion

Conclusion

References

[1] Richard Zhang, Phillip Isola, and Alexei A Efros. Colorful image colorization. In *European Conference on Computer Vision*, pages 649–666. Springer, 2016.

[2] Zezhou Cheng, Qingxiong Yang, and Bin Sheng. Deep colorization. In *Proceedings of the IEEE International Conference on Computer Vision*, pages 415–423, 2015.

[3] Aurelie Bugeau, Vinh-Thong Ta, and Nicolas Papadakis. Variational exemplar-based image colorization. *IEEE Transactions on Image Processing*, 23(1):298–307, 2014.

[4] Huimin Lu, Yujie Li, and Seiichi Serikawa. Underwater image enhancement using guided trigonometric bilateral filter and fast automatic color correction. In *Image Processing (ICIP), 2013 20th IEEE International Conference on*, pages 3412–3416. IEEE, 2013.

[5] Luz A Torres-Méndez and Gregory Dudek. Color correction of underwater images for aquatic robot inspection. In *International Workshop on Energy Minimization Methods in Computer Vision and Pattern Recognition*, pages 60–73. Springer, 2005.

[6] Guillaume Charpiat, Matthias Hofmann, and Bernhard Schölkopf. Automatic image colorization via multimodal predictions. *Computer Vision–ECCV 2008*, pages 126–139, 2008.

[7] Qing Luan, Fang Wen, Daniel Cohen-Or, Lin Liang, Ying-Qing Xu, and Heung-Yeung Shum. Natural image colorization. In *Proceedings of the 18th Eurographics conference on Rendering Techniques*, pages 309–320. Eurographics Association, 2007.

[8] Vadim Konushin and Vladimir Vezhnevets. Interactive image colorization and recoloring based on coupled map lattices. In *Graphicon2006 conference proceedings, Novosibirsk Akademgorodok, Russia*, pages 231–234, 2006.

[9] Yann LeCun, Yoshua Bengio, and Geoffrey Hinton. Deep learning. *Nature*, 521(7553):436–444, 2015.

[10] Anat Levin, Dani Lischinski, and Yair Weiss. Colorization using optimization. In *ACM Transactions on Graphics (ToG)*, volume 23, pages 689–694. ACM, 2004.

[11] Przemyslaw Lagodzinski and Bogdan Smolka. Digital image colorization based on probabilistic distance transformation. In *ELMAR, 2008. 50th International Symposium*, volume 2, pages 495–498. IEEE, 2008.

[12] Domonkos VARGA and Tamás Szirányi. Fully automatic image colorization based on convolutional neural network. *4th Winter School of PhD Students in Informatics and Mathematics*, page 36, 2016.

[13] Jie Li, Katherine A Skinner, Ryan M Eustice, and Matthew Johnson-Roberson. Watergan: Unsupervised generative network to enable real-time color correction of monocular underwater images. *arXiv preprint arXiv:1702.07392*, 2017.

[14] Erik Reinhard, Michael Adhikhmin, Bruce Gooch, and Peter Shirley. Color transfer between images. *IEEE Computer graphics and applications*, 21(5):34–41, 2001.

[15] Michael J Vrhel and HJ Trussell. Color correction using principal components. *Color Research & Application*, 17(5):328–338, 1992.

[16] Aditya Deshpande, Jason Rock, and David Forsyth. Learning large-scale automatic image colorization. In *Proceedings of the IEEE International Conference on Computer Vision*, pages 567–575, 2015.

[17] Vinod Nair and Geoffrey E Hinton. Rectified linear units improve restricted boltzmann machines. In *Proceedings of the 27th international conference on machine learning (ICML-10)*, pages 807–814, 2010.

[18] Sergey Ioffe and Christian Szegedy. Batch normalization: Accelerating deep network training by reducing internal covariate shift. *arXiv preprint arXiv:1502.03167*, 2015.

[19] Celeba dataset. `http://mmlab.ie.cuhk.edu.hk/projects/CelebA.html`. Accessed: 04-20-2017.

[20] Places2 dataset. `http://places2.csail.mit.edu/download.html`. Accessed: 04-20-2017.

[21] Jia Deng, Wei Dong, Richard Socher, Li-Jia Li, Kai Li, and Li Fei-Fei. Imagenet: A large-scale hierarchical image database. In *Computer Vision and Pattern Recognition, 2009. CVPR 2009. IEEE Conference on*, pages 248–255. IEEE, 2009.

[22] Martín Abadi, Ashish Agarwal, Paul Barham, Eugene Brevdo, Zhifeng Chen, Craig Citro, Greg S Corrado, Andy Davis, Jeffrey Dean, Matthieu Devin, et al. Tensorflow: Large-scale machine learning on heterogeneous distributed systems. *arXiv preprint arXiv:1603.04467*, 2016.